Supplemental Information

Self-organizing hair peg-like structures from dissociated skin progenitor cells: New insights for human hair follicle organoid engineering and Turing patterning in an asymmetric morphogenetic field

Erin L. Weber, M.D., Ph.D.[1,2]
Thomas E. Woolley, Ph.D.[3]
Chao-Yuan Yeh, M.D.[1]
Kuang-Ling Ou, M.D.[1,4,5]
Philip K. Maini, Ph.D.[6]
Cheng-Ming Chuong, M.D., Ph.D.[1,7, *]

[1] Department of Pathology, Keck School of Medicine of the University of Southern California, Los Angeles, CA
[2] Division of Plastic and Reconstructive Surgery, Keck School of Medicine of the University of Southern California, Los Angeles, CA
[3] Cardiff School of Mathematics, Cardiff University, Senghennydd Road, Cardiff, CF24 4AG, UK.
[4] Ostrow School of Dentistry of the University of Southern California, Los Angeles, CA
[5] Division of Plastic and Reconstructive Surgery, Department of Surgery, Tri-Service General Hospital, National Defense Medical Center, Taipei, Taiwan
[6] Wolfson Centre for Mathematical Biology, Mathematical Institute, Oxford, OX2 6GG, UK.
[7] Integrative Stem Cell Center, China Medical University, Taichung, Taiwan

Corresponding author: Cheng-Ming Chuong, M.D., Ph.D.
Keck School of Medicine of the University of Southern California
2011 Zonal Ave, HMR 313B
Los Angeles, CA 90089
cmchuong@usc.edu

Table of contents:

Supplemental Methods

Tissues and cells

Neonatal foreskin was obtained from the Cooperative Human Tissues Network (Nashville, TN). Second trimester fetal scalp skin, 17-19 weeks estimated gestational age (EGA), was obtained from Novogenix, Inc. (Los Angeles, CA) or Advanced Bioscience Resources (Alameda, CA). The tissues were incubated in 0.5% dispase overnight at 4°C. The epidermis and dermis were then mechanically separated using fine forceps and incubated in 0.35% collagenase I at 37°C for 30 minutes with occasional mixing. FBS was added to stop digestion. The epidermal and dermal cells were released from the surrounding matrix by pipetting with a glass pipette. The cells were passed through a 70 μm filter and centrifuged at 180xg for 5 minutes to remove debris. The epidermal cells were resuspended and cultured in CnT-PR medium (ZenBio) with penicillin, streptomycin, and amphotericin B (P/S/A) on plates treated with Coating Matrix (Life Technologies). Media was replaced every 4 days and cells were split at 80% confluency for a maximum of 4 weeks. The dermal cells were incubated in RBC lysis buffer (154 mM NH_4Cl, 10 mM $KHCO_3$, 0.1 mM EDTA, pH 7.2) at room temperature for 5 minutes and recentrifuged. RBC lysis was repeated once if needed and the cell pellet was washed with 1xPBS, resuspended in DMEM (Corning, 10-013), and kept at 4°C briefly before use the same day.

In vitro hair follicle reconstitution assay

$2x10^6$ neonatal foreskin keratinocytes and $3x10^6$ fetal scalp dermal cells were resuspended in 120 μl of F12:DMEM (1:1) medium (Gibco Ham's F-12 Nutrient Mix, ThermoFisher; DMEM, Corning) with 5% FBS and P/S/A for a final volume of 140 μl and plated as a droplet on a 6-well cell culture insert set into a matching 6-well plate (Falcon). 1.8 ml of 1:1 medium was added to the well. The droplets were incubated at 37°C and 5% CO_2 for 4-7 days. Growth factors were added to the culture droplet at the following concentrations daily: 1 μg/ml and 10 μg/ml sonic hedgehog (Shh, recombinant human, Peprotech), 0.5 μg/ml transforming growth factor beta 2 (Tgfβ2, recombinant human, Millipore), 1 μM retinoic acid receptor (RAR) antagonist ER 50891 (R&D Systems), 1 μg/ml fibroblast growth factors (FGF) 2, 7, and 10 (recombinant human, Miltenyi, Life Technologies, R&D Systems, respectively), 1 μg/ml Wnt7a (human recombinant, R&D Systems), 660 nM chelerythrine chloride and 10 nM bisindolylmaleimide I protein kinase inhibitors (PKCi, Millipore), 1 μg/ml and 10 μg/ml Noggin (human recombinant, Peprotech), 10 μg/ml Dkk1 (human recombinant, R&D Systems). 4% PFA or 100%

methanol was added directly to the cell insert and well to fix the droplet cultures overnight at 4°C for immunostaining.

Patch assay

$2x10^6$ neonatal foreskin keratinocytes and $3x10^6$ fetal scalp dermal cells were resuspended in 50 µl F12:DMEM (1:1) with 5% FBS and injected subcutaneously into the deep dermis of 6-12 week old hairless nude mice (NU/NU, Charles River). The nude mice were housed under standard conditions and were sacrificed for biopsy at 8 weeks post-injection. This protocol complied with ethical regulations regarding animal experimentation and was approved by the University of Southern California IACUC committee.

Immunostaining

Immunostaining was performed on fixed droplet cultures as whole mount specimens or paraffin-embedded sections. Antibodies are listed in Table S1. Images were taken with Zeiss LSM 510meta and 780 confocal microscopes.

Lentiviral vectors

The following vector genome plasmids were cloned from the stock plasmid pCCL-MU3-IRES-eGFP (courtesy of Paula Cannon, USC): pCCL-EF1α-GAP-eGFP, pCCL-K14-H2B-mOrange2, pCCL-MU3-H2B-mOrange2, pCCL-MU3-H2B-mCerulean3, and pCCL-p63-H2B-eGFP. Promoters and fluorescent proteins were amplified from human genomic DNA or plasmids purchased from Addgene. Primers are listed in Table S2.

293T cells at 50-60% confluency were transfected with 10 µg vector genome plasmid, 10 µg of packaging construct ΔR8.2 (P. Cannon, USC), and 2 µg envelope plasmid pCMV-VSVG (P. Cannon, USC) using the calcium phosphate method.[57] 10mM sodium butyrate was added to fresh media 16 hours post-transfection and removed after 8 hours. Virus-containing media was collected at 36 hours post-transfection, sterile filtered, and ultracentrifuged on a 20% sucrose cushion at 25,000 rpm and 4°C for 1.5 hours before storing at -20°C for up to 30 days or -70°C indefinitely.

Human neonatal foreskin keratinocytes were transduced with lentiviral vector, which was removed 4-8 hours later. The foreskin keratinocytes were cultured for at least 2 weeks before fluorescence could be strongly visualized. 10 µl virus was added directly to the *in vitro* hair reconstitution assay droplet at the time of plating for transduction of dermal cells.

Live cell imaging

Live cell confocal imaging was performed after 72 hours of culture. The cell culture insert membrane, including the culture droplet with transduced cells, was removed from the insert frame, suspended between silicone columns, and held in place with magnets inside a 6-cm glass-bottom cell culture dish (Electron Microscopy Sciences, 70674-52) modified with a glass coverslip inserted into the lid to place the cells at the appropriate focal distance for confocal or two-photon imaging. The entire volume of the culture dish was filled with hair follicle reconstitution assay medium and the dish was sealed with silicone caulk to maintain a lentivirus-free outer surface. The culture was imaged on a Zeiss LSM 5 Pascal microscope with a heated stage set to 37°C. A z-stack image was collected every 10 minutes.

Software analysis

Confocal images were processed with ImageJ software. Z-stack confocal images and live cell imaging z-stack series were converted into videos using Bitplane's Imaris software.

Statistical analysis

The statistical significance of differences in means was calculated using a two-sample T-test. Variance was calculated using the F-test. A p-value of <0.05 was considered significant. All error bars represent standard error of the mean. All experiments were performed in triplicate, at a minimum.

Mathematical modeling

We use the following reaction-diffusion model to simulate the interactions of two, as yet, experimentally unidentified, different morphogen populations, denoted u and v. Because of their roles in the equations u is termed the activator (existence of u promotes the production of more u and v) and v is termed the inhibitor (existence of v causes a reduction in the production of u). In turn, the cells read the local concentrations of the activator and inhibitor and determine their fate accordingly. The simulations take place on a circular two-dimensional domain of radius 10, centred at the orgin. We define the standard polar distance from the origin, r, in terms of the Cartesian coordinates (x, y) as $r = \sqrt{x^2 + y^2}$. The equations are, thus,

$$\frac{\partial u}{\partial t} = D_u \nabla^2 u + P_u \frac{u^2}{u^2 + k_1^2} \frac{1}{1 + G(r,t)v} - u,$$

$$\frac{\partial v}{\partial t} = D_v \nabla^2 v + P_v \frac{u^2}{u^2 + k_2^2} + s_v - v,$$

$$\frac{\partial u}{\partial n} = 0 = \frac{\partial v}{\partial n} on the boundary,$$

$$G(r,t) = \begin{cases} \alpha + r\beta t, & 0 \le t < t_f, \\ \alpha + r\beta t_f, & t \ge t_f. \end{cases}$$

In addition to the standard reaction-diffusion framework we have included a linear spatiotemporal gradient G. The gradient is radially symmetric; it starts flat at time zero and slowly increases at the boundary over time. At time t_f the gradient reaches its maximum value and freezes allowing the simulation to relax to a final heterogeneous steady state. This gradient modulates the inhibitor effect of the morphogen v on u, maximising its effect on the boundary.

Additional parameter values are given in Table S3. All unit dimensions are arbitrary, but consistent. The initial conditions for all populations were uniform random numbers with mean set to the largest positive uniform steady state when $t = 0$, and, hence, $G = \alpha$. The equations were simulated using a finite element Runge-Kutta method and the domain was discretised into 25970 domain elements. Note that the boundary conditions are specified to be zero-flux conditions, meaning that no substances are able to leak out of the domain. Initially, the time step was 10^{-3}, which was decreased as required to satisfy a relative step error tolerance of 10^{-6}. After a simulation was completed the simulation was repeated with double the initial domain elements and half the time step to guarantee convergence, through observing that the result did not change.

Supplemental Figures, Movies, and Tables

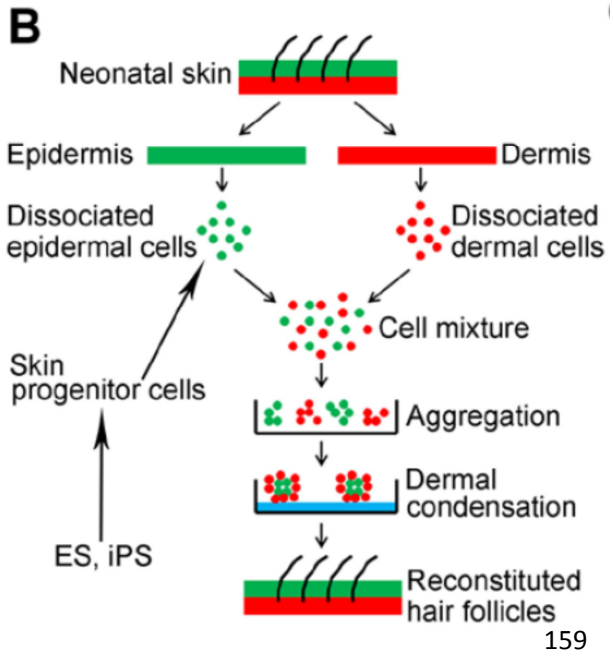

Figure S1. A generic working model for planar skin reconstitution with hair formation. Epidermal and dermal cells are mixed and plated on tissue culture insert in high cell density as a droplet. Different epidermal and dermal cells can be used, those derive from newborn skin, adult skin, adult hair follicle, and ES or iPS derived cells.

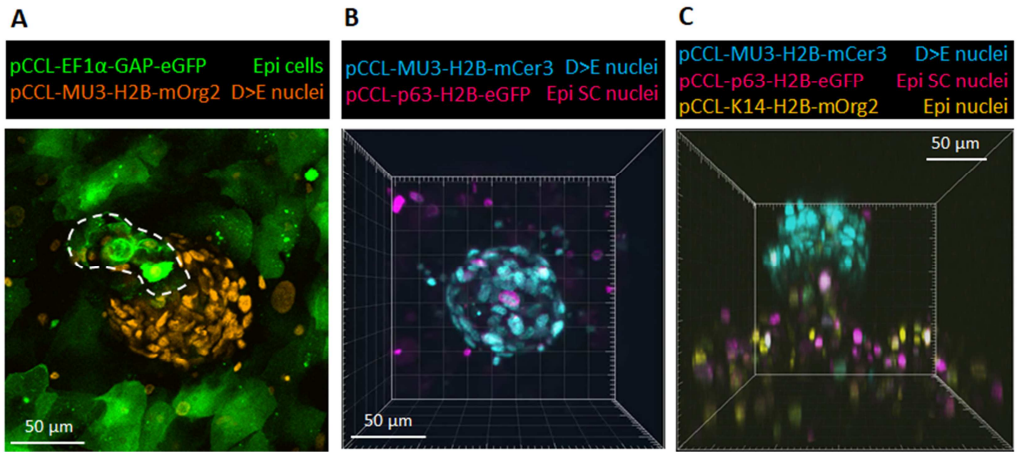

Figure S2. Live cell imaging of hair peg-like structures.

A. Overexpression of fluorescent proteins did not affect the ability to form hair peg-like structures. In this image, epidermal cell nuclei were marked with green fluorescent protein and dermal cell nuclei were preferentially marked with orange fluorescent protein. The dotted line outlines the epidermal stalk. Epi = epidermal, D = dermal, E = epidermal. (n=7)

B. A still image from a two-color live imaging video (Fig. S5A), looking down from the top of the culture droplet, demonstrates a dermal cap. p63-positive keratinocyte nuclei are magenta, dermal cell nuclei are cyan. Epi SC = epidermal stem cell. (n=5)

C. A single lateral image taken from a three-color live imaging video (Fig. S5B) demonstrates a hair peg-like structure. Keratinocyte nuclei are orange, p63-positive keratinocyte nuclei are magenta, and dermal cell nuclei are cyan. (n=5)

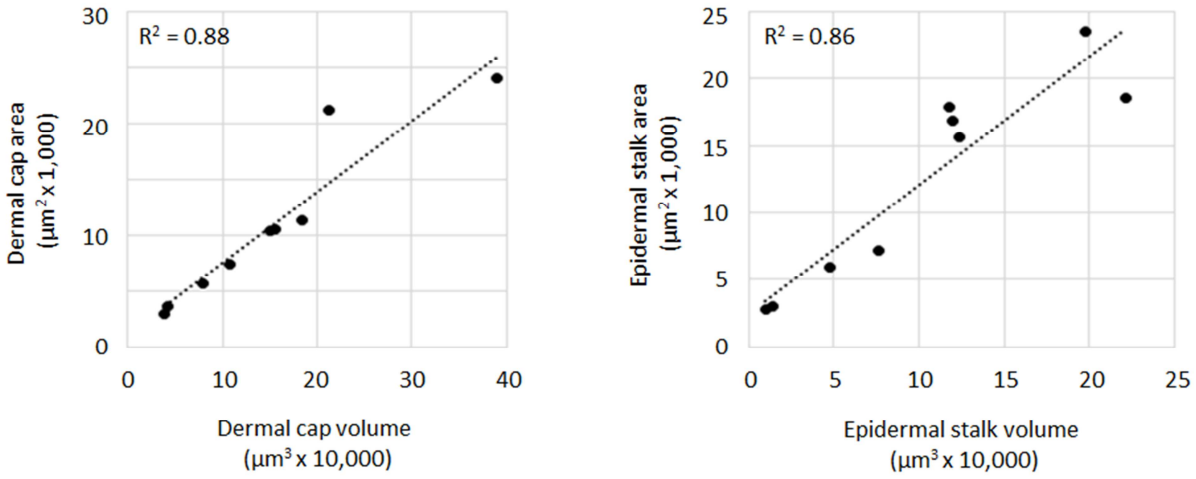

Figure S3. Reconstituted hair peg-like structures displayed radial symmetry.

Cap and stalk sagittal areas maintained a linear relationship with the total cap and stalk volumes, emphasizing the radial symmetry of these structures and allowing us to simplify analysis by measuring the area of each structure at the midpoint corresponding to maximal width.

Movie S1. Three-dimensional z-stack reconstructions of human hair peg-like structures formed in culture.

A. Whole mount confocal z-stack images of multiple hair peg-like structures immunostained with keratin-14 (green), vimentin (red), and TO-PRO-3 iodide (nuclei, blue) demonstrate the periodic patterning and formation of distinct structures within a 425 μm^2 area. Cells within the keratinized sheet were difficult to stain with pancytokeratin due to poor antibody penetration.

B. Whole mount confocal z-stack images of hair peg-like structures immunostained with pancytokeratin (green) and propidium iodide (nuclei, red) demonstrate the spherical configuration of the dermal cap and the tubular structure of the epidermal stalk. Sandwiching of the whole mount culture beneath a coverslip for confocal imaging caused the hair pegs to appear bent or flattened against the keratinocyte sheet.

C. Higher magnification view of a single reconstituted human hair peg-like structure immunostained with pancytokeratin (green) and propidium iodide (nuclei, red). Note epidermal cells start to wrap around the dermal cap.

Movie S2. Three-dimensional z-stack reconstructions of reconstituted human hair peg-like structures demonstrate markers of dermal papilla gene expression.

A. Whole mount confocal z-stack imaging demonstrates α-SMA staining in a central location within the dermal cap of a hair peg-like structure. α-SMA (green), propidium iodide (red).

B. Whole mount confocal z-stack imaging demonstrates the presence of extracellular collagen IV at the epidermal-dermal interface. CD34 - an early dermal papilla marker (green), collagen IV (red), TO-PRO-3 iodide (blue). The large green lobules are artifacts representing dead cells which have trapped the dye.

Movie S3. Three-dimensional z-stack reconstructions of epidermal placode-like structures and dermal clusters at 48 hours.

A. Whole mount confocal z-stack imaging demonstrates multiple dermal clusters atop a keratinocyte sheet and altered keratinocyte arrangement pattern around the dermal clusters. Pancytokeratin (green), propidium iodide (red). The large green lobules are artifacts representing dead cells which have trapped the dye.

B. Whole mount confocal z-stack imaging demonstrating vimentin-positive immunostaining of the dermal clusters at 48 hours post-plating. Vimentin (red), TO-PRO-3 iodide (blue).

Movie S4. Live cell imaging of a reconstituted human hair peg-like structure.

Time-lapse movie highlighting dermal cell shape and movement within the dermal cap of a reconstituted human hair peg-like structure, as viewed from the top of a culture droplet. The epidermal stalk is not visible in this view. A z-stack image was recorded every 10 minutes from 101-103 hours post-plating and is replayed at a rate of 5 frames per second. The entire culture descended along the z-axis during imaging, resulting in partial movement out of the focal plane over time. p63-positive epidermal cells were labelled with nuclear eGFP fluorescent protein (magenta). Dermal cells were labelled with nuclear mCerulean3 fluorescent protein (cyan). Note the varied dermal cell movement and nuclear shape within the dermal cap. Few p63-positive epidermal cells are visible in this top-down view, as the epidermal stalk is obscured by the cells of the dermal cap. However, reproducibly, 1-3 p63-positive epidermal cells were noted within the dermal cap, frequently at the apex, as seen here.

Movie S5. Live cell imaging of a reconstituted human hair peg-like structure.

Time-lapse movie of a reconstituted human hair peg-like structure, viewed from top-down (**A**) and lateral (**B**) orientations. A z-stack image was recorded every 10 minutes from 83-85 hours post-plating and is replayed at a rate of 10 frames per second. All epidermal nuclei were pre-labelled with mOrange2 fluorescent protein (yellow). p63-positive epidermal nuclei were labelled with eGFP (magenta). Dermal nuclei were labelled with mCerulean3 fluorescent protein (cyan). Note that the entire specimen drifts during imaging. However, the epidermal cells within the epidermal sheet remain static, as evidenced by no change in positional relationship with adjacent epidermal cells. The position of the dermal cap does move in space, relative to the epidermal sheet, because the epidermal stalk is flexible and sways within the droplet culture medium.

Movie S6. Mathematical simulation of human hair follicle periodic pattern formation *in vitro*.

The changes in periodic patterning from long stripes to short stripes to punctate clusters, corresponding to dermal clusters and then hair peg-like structures, is represented here by a Turing-based mathematical simulation. The periodic patterns form sequentially on the left, as the radially symmetric spatiotemporal gradient increases in the middle and right-sided diagrams.

286

287 **Table S1. Antibodies.**

Antibody	Source	Catalog Number	Dilution
Alkaline phosphatase	Abcam	ab108337	1:100
α-SMA	ThermoFisher	MA1-37028	undiluted
β-catenin	Sigma	C7207	1:100
CD34	Millipore	CBL496	1:100
Collagen I	Abcam	ab34710	1:100
Collagen III	Abcam	ab7778	1:100
Collagen IV	Abcam	ab19808	1:100
Cytokeratin 14/15/16/19 (pancytokeratin)	Becton Dickinson	550951	1:100
Keratin-10	ThermoFisher	MA5-11599	1:100
Keratin-14	ThermoFisher	MS-115-P1	1:100
Laminin 5	Abcam	ab14509	1:100
p63	Santa Cruz	Sc-8343	1:100
PCNA	Abcam	ab92552	1:100
Propidium iodide	Sigma	P4170	1:1000
TO-PRO-3 iodide	ThermoFisher	T3605	1:500
Vimentin	Cell Signaling	3390	1:100

Table S2. Primers for lentiviral vector construction

gDNA = genomic DNA

Sequence	Forward primer	Reverse primer	Amplified from	Source
EF1α promoter	ATAAATGAATTCGCTCCGGTGCCCGTCAG	GCCCAGGAATTCTCACGACACCTGAAATGG	plasmid RBW1	Chuong lab
p63 promoter	TTCGGGGCTAGCGTAAGTAGGTTTTTTTTT	TAAGCTGCTAGCGTTAGCTGTAAGATTGATC	Human gDNA	293T cells
K14 promoter	TTATATGAATTCCCCGGGCTCCGGAGCTTC	GCTGGGGAATTCCTCGGGTAAATTGGAAAG	Human gDNA	293T cells
H2B-mOrange2	TAGATTGCTAGCATGCCTGAACCC	TAAGATGCTAGCTCACTTGTACAGC	plasmid #57962	Addgene
GAP-eGFP	TAGATTGGATCCATGCTGTGCTGTATG	TAAGATGGATCCTTACTTGTACAGCTCG	plasmid #14757	Addgene
H2B-eGFP	TAAAATGCTAGCATGCCTGAGCCGGCCAAG	GCCCGAGCTAGCTTACTTGTACAGCTCGTC	RCAS-H2B-eGFP	Chuong lab
H2B-mCerulean3	TTTATTGCTAGCATGCCAGAGCCAGCGAAG	GGGTAGGCTAGCTTACTTGTACAGCTCGTC	plasmid #55374	Addgene

Table S3. Parameter values for equations (1)-(4).

Parameter	Value	Definition
P_u	1000	Strength of influence of activator on activator
P_v	100	Strength of influence of activator on inhibitor
k_1	10	Activator sensitivity to activator
k_2	10	Inhibitor sensitivity to activator
s_v	1	Inhibitor source
D_u	2.5×10^{-4}	Activator diffusion rate
D_v	1.25×10^{-2}	Inhibitor diffusion rate

α	1.1	Basal level of gradient
β	$1/250$	Rate of gradient increase
t_f	150	Time after which the gradient stops evolving

295